

Article

High-Precision Quality Prediction Based on Two-Dimensional Extended Windows

Luping Zhao * and Jiayang Yang

College of Information Science and Engineering, Northeastern University, Shenyang 110819, China; 20194179@stu.neu.edu.cn

* Correspondence: zhaolp@ise.neu.edu.cn; Tel.: +86-18842552385

Abstract: A PLS-based quality prediction method is proposed for batch processes using two-dimensional extended windows. To realize the adoption of information in the directions of sampling time and batch, a newly defined region of support (ROS), called the k - i -back-extended region of support (KIBROS), is proposed; it establishes an extended window by adding two regions of data to the traditional ROS to include all possible important data for quality prediction. Based on the new ROS, extended windows are established, and different models are proposed using the extended windows for batch process quality prediction. Furthermore, using the typical injection molding batch process as an example, the proposed quality prediction method is experimentally verified, proving that the proposed methods have higher prediction accuracy than the traditional method and that the prediction stability is also improved.

Keywords: batch process; partial least squares; extended window; quality prediction

MSC: 93-02



Citation: Zhao, L.; Yang, J.

High-Precision Quality Prediction Based on Two-Dimensional Extended Windows. *Mathematics* **2024**, *12*, 1396. <https://doi.org/10.3390/math12091396>

Academic Editor: Ivo Petráš

Received: 27 March 2024

Revised: 21 April 2024

Accepted: 29 April 2024

Published: 3 May 2024



Copyright: © 2024 by the authors. Licensee MDPI, Basel, Switzerland. This article is an open access article distributed under the terms and conditions of the Creative Commons Attribution (CC BY) license (<https://creativecommons.org/licenses/by/4.0/>).

1. Introduction

Precise variable prediction modeling depends on a good understanding of process characteristics. Industrial processes usually have characteristic changes in two directions. The first is the time direction within a production period, where the main conditions do not change, but some of them shift due to complex factors. During the production period, typically only one kind of production is provided. The characteristic changes in this direction lead to a series of phases. The second direction of change is the repeat production direction, where the main conditions can be maintained to obtain the same products, but the time-varying problem may still occur; however, the main conditions can be changed systematically to obtain different production types.

Multivariate statistical modeling methods are typical data-driven modeling methods, of which principal component analysis (PCA) [1] and partial least squares (PLS) [2] have been applied widely in the fields of industrial process modeling, monitoring, and control [3–5]. For batch processes, multilinear principal component analysis (MPCA) and multiway partial least squares regression (MPLS) are classic methods that address the three-dimensional matrix by unfolding it into a two-dimensional matrix [6,7]. Following their development, many research works have been presented [8–12]. Among them, some papers have focused on multiphase characteristics, where different statistical models are built for different phases [11,12]. Additionally, the relationships between phases were investigated for better modeling and prediction [13]. For both the continuous processes and the batch processes, the sliding window method is typically used to address the time-varying problem [12], and multiple models are usually built for multiple modes [14–17]. As mentioned above, the characteristic changes in the time direction and the repeat production direction have been topics of interest for researchers. However, these research works tend to deal with one problem each; that is, they tend to deal with the characteristic change

problems in only one direction. This makes it difficult to apply these methods because the characteristics usually change in the two directions simultaneously. Thus, it is necessary to investigate a uniform modeling method that can address characteristic changes in both directions simultaneously.

Recently, a complete set of process modeling methods was developed to solve the process characteristics evolution problem in both the intra-batch and inter-batch directions [18], where the problems in the two directions are firstly handled separately and then the two strategies are combined. This kind of approach is flexible for selecting appropriate modeling methods in the two directions, and new strategies can be developed based on the scheme [19]. However, the separation of the methods is unavoidable. It is difficult to provide a comprehensive explanation of process characteristics using two unrelated methods. In addition, when the methods for both directions need to be combined, the method structure is relatively complex and difficult to comprehend and implement. Additionally, the idea of tracing the evolution problem of the process characteristics in both the intra-batch and inter-batch directions was also adopted and combined with multimode analysis. A two-dimensional, two-layer quality regression model was established to monitor multiphase, multimode batch processes [20]. With this method, two-dimensional regression traces the intra-batch and inter-batch characteristics, while the two-layer structure establishes the relationship between the target process and the historical modes and phases. The two-layer structure is more suitable for multimode and multiphase characteristics but is not suitable for slow time-varying characteristics in the two directions. Therefore, it is necessary to develop a set of modeling strategies to trace the slow time-varying intra-batch and inter-batch characteristics simultaneously.

This paper presents a comprehensive and thorough analysis of the region of support (ROS). In this study, which considers industrial processes with slow time-varying characteristics in both the time direction and the repeat production direction, a modeling algorithm using two-dimensional extended windows is proposed for quality prediction. In a previous work [21], the ROS was defined as the data before the time point of the current batch and the previous batches, which include the data of the previous sampling times in the same batch (KROS) and the data of the previous sampling times in the historical batches (KIROS). In this paper, the ROS is redefined and extended to four sub-regions, including all the possible regions in the time direction and the batch direction, which include the data of the previous sampling times in the same batch (KROS), the data of the same sampling time in the historical batches (IROS), the data of the previous sampling times in the historical batches (KIROS), and the data of the later sampling times in the historical batches (BROS). The data of the previous batches and those of the previous sampling times are considered to be correlated with the current sampling data; thus, a more precise online prediction of product quality can be provided. On this basis, the i -extended window, k -extended window, i - k -extended window, back-extended window, and i - k -back-extended window are proposed. Finally, quality prediction models are constructed using the extended windows. The injection molding process is used as an example for experimental verification. Suggestions are given for the usage of the extended window-based quality prediction methods.

The remainder of this paper includes the following: In the second section, the quality prediction algorithm, the partial least squares (PLS) method, and the establishment of the sliding window are first introduced. Then, the modeling strategy with the extended ROS—specifically, the two-dimensional i - k -back-extended ROS—is proposed, followed by the quality prediction method and two evaluation indicators. The application of the proposed method to the injection modeling process is introduced in the third section. The fourth section presents the conclusion.

2. Methodology

2.1. Partial Least Squares (PLS) Method

PLS is a classical regression method for quality prediction in industrial processes. It not only carries out regression modeling but also simplifies the structure of the data and

analyzes the correlation between two groups of variables [16,22]. Using the PLS algorithm, the correlations between the process variables and the quality variables can be transformed into a latent variable space for research. It should be noted that the inputs for PLS should be two-dimensional matrices. PLS is a classical multivariate statistical method and is more suitable for addressing application backgrounds with fewer samples, like the injection molding process in this paper, compared to deep learning methods. PLS is efficient, and its prediction effect can meet the accuracy requirements; so, it was adopted in this work. Generally, deep learning methods require a large amount of data and are not suitable for processes with this background. However, a suitable deep learning method may be chosen as a substitute for processes with a large amount of data. For processes with limited data, a deep learning method with a reasonable algorithm may also be chosen as a substitute to address the limited data problem.

The main formula of PLS capturing the relationship between $\tilde{\mathbf{X}}$ and $\tilde{\mathbf{Y}}$ is as follows:

$$\begin{aligned}\tilde{\mathbf{X}} &= \mathbf{TP}^T + \mathbf{E} = \sum_{a=1}^A \mathbf{t}_a \mathbf{p}_a^T + \mathbf{E} \\ \tilde{\mathbf{Y}} &= \mathbf{UQ}^T + \mathbf{F} = \sum_{a=1}^A \mathbf{u}_a \mathbf{q}_a^T + \mathbf{F}\end{aligned}\quad (1)$$

where \mathbf{T} and \mathbf{U} represent the score matrices, \mathbf{P} and \mathbf{Q} represent the load matrices, and \mathbf{E} and \mathbf{F} represent the residual matrices.

The regression model based on PLS is as follows:

$$\tilde{\mathbf{Y}} = \tilde{\mathbf{X}}\mathbf{B}\quad (2)$$

where \mathbf{B} is the regression coefficient matrix.

2.2. Establishment of Sliding Window

For a typical batch process, the process data are often stored in the form of a three-dimensional matrix, which is denoted as $\bar{\mathbf{X}}(I \times J_x \times K)$, where I represents the number of batches, J_x represents the number of process variables, and K represents the number of sampling points in a batch. Meanwhile, at the end of one batch operation, the quality data can be obtained, which are stored in the form of a two-dimensional matrix, denoted as $\bar{\mathbf{Y}}(I \times J_y)$, where J_y represents the number of quality variables. Usually, a batch process needs to be divided into several phases using some of the production knowledge of the specific process, and the critical-to-quality phases and critical-to-quality variables are identified. These phases are then treated separately. Within the phases, the slow time-varying problem is characterized by the relationship change between the process variables and the quality variables from batch to batch. The key step of the analysis is to divide the slow time-varying batch process into different modes and to build different models for them. The sliding window method was adopted in this study; a demonstration diagram is shown in Figure 1. In the figure, I represents the batch direction, j represents the process variable direction, and k represents the direction of the sampling points in a batch. The first window is established using the process data of the first I_w batch, where the process variable matrix is denoted as $\mathbf{X}(I_w \times J_x \times K)$ and the corresponding quality data are denoted as $\mathbf{Y}(I_w \times J_y)$. When sliding, the window moves down by L batches each time; that is, the second window is formed using the data of the $(L + 1)$ -th to the $(L + I_w)$ -th batches. It is advised that L be made 1 [23].

The process data in the sliding window can be divided into K time slices, and the k -th can be represented as $\mathbf{X}_k(I_w \times J_x)$. Traditionally, a PLS model can be built between the time-slice data \mathbf{X}_k and the quality data \mathbf{Y} . Next, each element in the time-slice data \mathbf{X}_k , $\mathbf{x}_{i,k}(1 \times J_x)$, is extended using novel ROSSs.

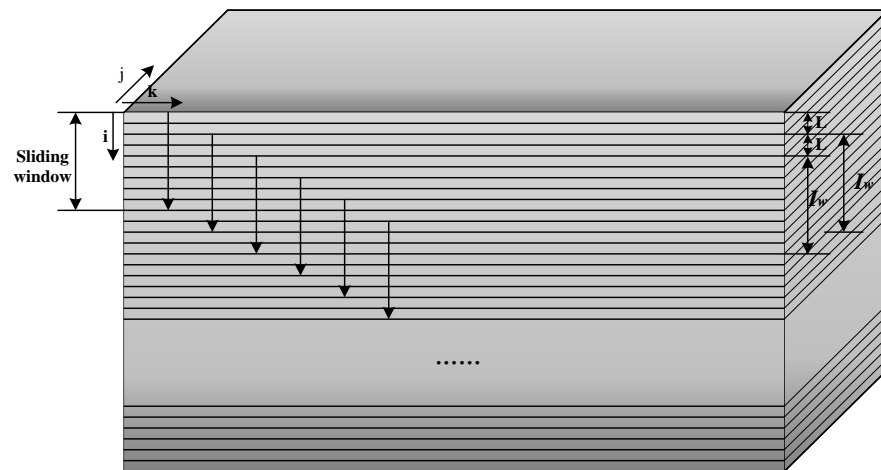


Figure 1. Schematic diagram of sliding window.

2.3. Two-Dimensional Extended ROS

The schematic diagram of the ROS proposed in this paper is shown in Figure 2. For convenience, for the process data, $\mathbf{X}(I_w \times J_x \times K)$, the variable direction is not shown in the figure, and each white circle represents a sample point $\mathbf{x}_{i,k}(1 \times J_x)$. The previous neighbors of $\mathbf{x}_{i,k}$ may affect it, including not only past points in the time direction, $\mathbf{x}_{i,k-1}, \mathbf{x}_{i,k-2}, \dots, \mathbf{x}_{i,1}$, but also past points in the batch direction, $\mathbf{x}_{i-1,k}, \mathbf{x}_{i-2,k}, \dots, \mathbf{x}_{1,k}$, past points in both the time direction and the batch direction, $\mathbf{x}_{i-1,k-1}, \mathbf{x}_{i-1,k-2}, \dots, \mathbf{x}_{i-1,1}, \mathbf{x}_{i-2,k-1}, \dots, \mathbf{x}_{i-2,1}, \dots, \mathbf{x}_{1,1}$, and even past points of the past batches but with time indexes larger than k , $\mathbf{x}_{i-1,k+1}, \mathbf{x}_{i-1,k+2}, \dots, \mathbf{x}_{i-1,K}, \mathbf{x}_{i-2,k+1}, \dots, \mathbf{x}_{i-2,K}, \dots, \mathbf{x}_{1,k+1}, \dots, \mathbf{x}_{1,K}$. The region covering the above points which may influence the contribution of the current point to the final quality is defined as the novel ROS. Thus, these four sub-regions of data are called the k -extended region of support (KROS), the i -extended region of support (IROS), the k - i -extended region of support (KIROS), and the back-extended region of support (BROS). Their specific locations are shown in Figure 2. The novel k - i -back-extended region of support (KIBROS) includes the above four ROSs.

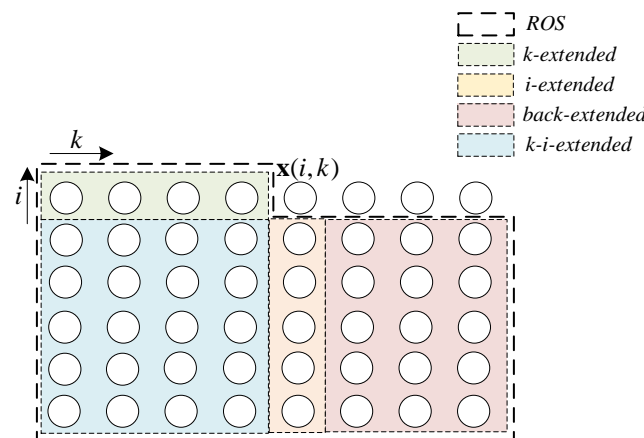


Figure 2. Schematic diagram of novel ROS.

In the cited paper [21], the ROS was defined as the data before the time point of the current batch and previous batches, including the k -extended and k - i -extended ROSs in Figure 2. That is, in the previous work, only the two parts on the left side of Figure 2 were defined as ROSs. In this paper, the ROS is redefined and extended to four sub-regions, including all the possible regions in the time direction and the batch direction. Correspondingly, the observed element $\mathbf{x}_{i,k}$ is extended to the four specific ROSs.

In previous batch process research, the variable data of the k -th sampling time in each batch were formed into a time-slice matrix, $\mathbf{X}_k(I \times J_x)$, and used to determine the relationship between the sampling process data and the quality data. Then, all the time-slice matrices were used to obtain the final prediction quality [24]. In this work, all the samples in the ROSs were considered at the same time when each sampling point was modeled. Thus, the established model contains the corresponding information, and the prediction accuracy can be further improved. Based on the above data in the ROSs, a two-dimensional extended matrix is proposed, whose specific description is as follows.

Step 1. Extension of the samples in the k -extended region of support (KROS).

The past points in the time direction; that is, the samples in the KROS, $\mathbf{x}_{i,k-1}, \mathbf{x}_{i,k-2}, \dots, \mathbf{x}_{i,1}$, were used to construct the extended ROS in the time direction. And the extended process data matrix can be obtained as shown below, while the quality data vector remains since it represents the final quality for the whole batch. It should be noted that for the final quality, which can only be obtained at the end of each batch process, the k index is not necessary.

$$\mathbf{x}_{i,k}^F = [\mathbf{x}_{i,k-F+1}, \dots, \mathbf{x}_{i,k-1}, \mathbf{x}_{i,k}] \tag{3}$$

$$\mathbf{y}_i^F = \mathbf{y}_i \tag{4}$$

where F represents the total number of sampling times included; in other words, a total of $F - 1$ sampling times are extended forward.

Step 2. Extension of the samples in the i -extended region of support (IROS).

The following is the method used to build the extended ROS in the batch direction. For the variable vector of the i -th batch at the k -th sampling time, $\mathbf{x}_{i,k}(1 \times J)$, the variable vector of the $(i-1)$ -th batch, $\mathbf{x}_{i-1,k}$, is spliced at the back of $\mathbf{x}_{i,k}$, and the variable vectors of the $(i-2)$ -th, $(i-3)$ -th, ..., $(i-N+1)$ -th batches are spliced behind the matrix in turn, where N is the number of batches included. The extended process variable matrix is shown below, and similarly, the quality matrix is established.

$$\mathbf{X}_{i,k}^N = \begin{bmatrix} \mathbf{x}_{i,k} \\ \mathbf{x}_{i-1,k} \\ \vdots \\ \mathbf{x}_{i-N+1,k} \end{bmatrix} \tag{5}$$

$$\mathbf{Y}_i^N = \begin{bmatrix} \mathbf{y}_i \\ \mathbf{y}_{i-1} \\ \vdots \\ \mathbf{y}_{i-N+1} \end{bmatrix} \tag{6}$$

Step 3. Extension of the samples in the k - i -extended region of support (KIROS).

Combining the previously proposed KROS and the IROS, the subsequently proposed method can further realize the construction of a two-dimensional extended matrix based on the time-batch evolution information.

First, for the i -th batch, the data are extended in the direction of the sampling time according to the method mentioned in Step 1 to obtain a matrix $\mathbf{x}_{i,k}^F$.

Then, the i -th to the $(i - N + 1)$ -th batches in the IROS are extended according to the time direction, and the following extended process data matrix is obtained, as well as the extended quality data matrix:

$$\mathbf{X}_{i,k}^{F,N} = \begin{bmatrix} \mathbf{x}_{i,k-F+1} & \cdots & \mathbf{x}_{i,k-1} & \mathbf{x}_{i,k} \\ \mathbf{x}_{i-1,k-F+1} & \cdots & \mathbf{x}_{i-1,k-1} & \mathbf{x}_{i-1,k} \\ \vdots & \ddots & \vdots & \vdots \\ \mathbf{x}_{i-N+1,k-F+1} & \cdots & \mathbf{x}_{i-N+1,k-1} & \mathbf{x}_{i-N+1,k} \end{bmatrix} \tag{7}$$

$$Y_i^{F,N} = \begin{bmatrix} y_i \\ y_{i-1} \\ \vdots \\ y_{i-N+1} \end{bmatrix} \tag{8}$$

Step 4. Extension of the samples in the back-extended region of support (BROS).

Since, in the above work, only the data before the k -th sample time were adopted, it was necessary to further consider the data information after the k -th sample time to further improve the accuracy of the quality prediction. The construction method for the backward extended matrix is symmetric with the two-dimensional extended matrix based on the time-batch evolution information proposed in the previous step. In addition, since it is not possible to obtain the information of the current i -th batch after the k -th sample time during modeling, and considering the similarity of the processes between batches in the batch process, the data after the k -th time of the $(i-1)$ -th batch are used as an alternative; then, the corresponding position of the current batch is filled. A schematic diagram of the specific process is shown in Figure 3. In this figure, different batches are represented by different colors and since the I -th batch is the same with the $(I-1)$ -th batch, the same color is used for them.

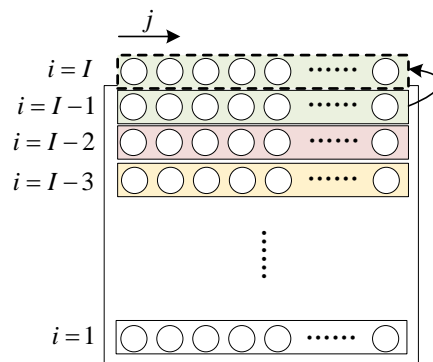


Figure 3. Backward extension in the direction of the batch.

A backward extended process data matrix and a backward extended quality data matrix can be constructed using the abovementioned method in the batch and sampling time directions, as shown below:

$$X_{i,k}^B = \begin{bmatrix} x_{i-1,k+1} & x_{i-1,k+2} & \cdots & x_{i-1,k+B} \\ x_{i-1,k+1} & x_{i-1,k+2} & \cdots & x_{i-1,k+B} \\ x_{i-2,k+1} & x_{i-2,k+2} & \cdots & x_{i-2,k+B} \\ \vdots & \vdots & \ddots & \vdots \\ x_{i-N+1,k+1} & x_{i-N+1,k+2} & \cdots & x_{i-N+1,k+B} \end{bmatrix} \tag{9}$$

$$Y_i^B = \begin{bmatrix} y_i \\ y_{i-1} \\ y_{i-2} \\ \vdots \\ y_{i-N+1} \end{bmatrix} \tag{10}$$

where B is the number of backward samples included.

Step 5. Extension of the samples in the k - i -back-extended region of support (KIBROS).

Using sampled data from the whole range of ROSSs, a method for constructing a k - i -back-extended matrix based on time-batch evolution information is subsequently proposed. First, the process data at the k -th sampling time in the i -th batch currently considered, $x_{i,k}$, are extended in the direction of the sampling time to obtain $X_{i,k}^{F,N,B}$, expressed as Equation (11), followed by the quality data:

$$\mathbf{X}_{i,k}^{F,N,B} = \begin{bmatrix} \mathbf{x}_{i,k-F+1} & \cdots & \mathbf{x}_{i,k-1} & \mathbf{x}_{i,k} & \mathbf{x}_{i-1,k+1} & \mathbf{x}_{i-1,k+2} & \cdots & \mathbf{x}_{i-1,k+B} \\ \mathbf{x}_{i-1,k-F+1} & \cdots & \mathbf{x}_{i-1,k-1} & \mathbf{x}_{i-1,k} & \mathbf{x}_{i-1,k+1} & \mathbf{x}_{i-1,k+2} & \cdots & \mathbf{x}_{i-1,k+B} \\ \vdots & \ddots & \vdots & \vdots & \vdots & \vdots & \ddots & \vdots \\ \mathbf{x}_{i-N+1,k-F+1} & \cdots & \mathbf{x}_{i-N+1,k-1} & \mathbf{x}_{i-N+1,k} & \mathbf{x}_{i-N+1,k+1} & \mathbf{x}_{i-N+1,k+2} & \cdots & \mathbf{x}_{i-N+1,k+B} \end{bmatrix} \quad (11)$$

$$\mathbf{Y}_i^{F,N,B} = \begin{bmatrix} \mathbf{y}_i \\ \mathbf{y}_{i-1} \\ \vdots \\ \mathbf{y}_{i-N+1} \end{bmatrix} \quad (12)$$

The parameters that determine the size of the expanded matrix are F , N , and B , as mentioned above. During actual construction, these three parameters can be determined one by one to achieve the best prediction effect.

As previously mentioned, the quality prediction model is built between the time-slice data \mathbf{X}_k and the quality data \mathbf{Y} . In this work, each element in the time-slice data \mathbf{X}_k , $\mathbf{x}_{i,k} (1 \times J_x)$, was extended using the proposed $\mathbf{x}_{i,k}^F$, $\mathbf{x}_{i,k}^N$, $\mathbf{x}_{i,k}^{F,N}$, $\mathbf{x}_{i,k}^B$, and $\mathbf{x}_{i,k}^{F,N,B}$, according to the proposed new ROs, obtaining the extended time-slice data $\mathbf{X}_{k,ex}$. Similarly, each element in the quality data \mathbf{Y} , \mathbf{y}_i , was extended using the proposed \mathbf{y}_i^F , \mathbf{y}_i^N , $\mathbf{y}_i^{F,N}$, \mathbf{y}_i^B , and $\mathbf{y}_i^{F,N,B}$, obtaining the extended quality data \mathbf{Y}_{ex} . Subsequently, the quality prediction model was built.

2.4. Quality Prediction Method and Evaluation Indicators

Following the construction of the extended data matrix within each sliding window, PLS was used to finish the quality prediction. As mentioned above, the PLS model based on an extended window is expressed as follows:

$$\begin{aligned} \mathbf{X}_{c,k,ex} &= \mathbf{T}_{c,k,ex} \mathbf{P}_{c,k,ex}^T + \mathbf{E}_{c,k,ex} = \sum_{a=1}^A t_{c,k,ex,a} \mathbf{p}_{c,k,ex,a}^T + \mathbf{E}_{c,k,ex} \\ \mathbf{Y}_{c,ex} &= \mathbf{U}_{c,k,ex} \mathbf{Q}_{c,k,ex}^T + \mathbf{F}_{c,k,ex} = \sum_{a=1}^A u_{c,k,ex,a} q_{c,k,ex,a}^T + \mathbf{F}_{c,k,ex} \end{aligned} \quad (13)$$

where $\mathbf{X}_{c,k,ex}$ represents the extended time-slice data matrices, $\mathbf{Y}_{c,ex}$ represents the extended quality data matrices, and c represents the c -th phase for the multiphase processes. The regression model is as follows:

$$\mathbf{Y}_{c,ex} = \mathbf{X}_{c,k,ex} \mathbf{B}_{c,k,ex} \quad (14)$$

For the batch whose quality is predicted online, the process variable matrix is denoted as \mathbf{X}_k^* . The extended matrix of this test batch was established using the method proposed in Section 2.3, denoted as $\mathbf{X}_{c,k,ex}^*$ and it was substituted into the following formula to obtain the prediction quality.

$$\tilde{\mathbf{Y}}_{c,k,ex} = \mathbf{X}_{c,k,ex}^* \mathbf{B}_{c,k,ex} \quad (15)$$

A few indicators were used to evaluate the performance of the prediction methods based on the model. The prediction accuracy, $R_{k,c}^2$, of the quality prediction model of the k -th sampling time within the c -th phase was calculated as follows:

$$R_{k,c}^2 = \frac{\sum_{i=1}^I (\tilde{y}_{i,c,k,ex} - \bar{y})^2}{\sum_{i=1}^I (y_i - \bar{y})^2} \quad (16)$$

where y_i is the measured value of the quality variable of the i -th batch, $\tilde{y}_{i,c,k,ex}$ is the predicted value of one of the quality variables of the k -th sampling time within the c -th phase, and \bar{y} is the average value of the quality variable measured at the end of the i -th

batch. The value range of $R_{k,c}^2$ is 0–1. If $R_{k,c}^2$ approaches 1, it indicates that the precision of the quality prediction model is high. If $R_{k,c}^2$ approaches 0, it means that the change in this phase does not explain the change in quality well.

Furthermore, $\overline{R_c^2}$ is proposed to indicate the average impact of the c -th phase:

$$\overline{R_c^2} = \sum_{k=k_{start}}^{k_{end}} R_{k,c}^2 / (k_{end} - k_{start}) \tag{17}$$

where k_{start} and k_{end} represent the starting and last sampling points in the c -th phase, separately. In this study, the offline quality analysis was carried out based on the comparison of $\overline{R_c^2}$ and $R_{k,c}^2$.

The root mean square error (RMSE) was used to verify the prediction accuracy of the model, which is expressed using the following formula:

$$RMSE = \sqrt{\sum_{i=1}^r d_i^2 / r} \tag{18}$$

where r is the number of measurement groups, and d_i is the deviation between one group of the predicted values and the real value of quality. As can be seen in the formula, the smaller the RMSE, the more accurate the prediction results. The comparison of the online prediction precision of each method was based on the evaluation of the RMSE.

3. Illustration and Discussion

3.1. Introduction of Injection Molding Process

Injection molding technology is an important plastic processing method, and the injection molding process is a typical batch process. During the injection molding process, there are often drifts in the operating conditions and other unknown perturbations that can lead to unstable product quality. Therefore, determining how to accurately predict the product quality to adjust the process parameters in time so that the product quality can meet the requirements is the basic research direction of quality control for the injection molding process. A schematic diagram of a typical injection molding machine is shown in Figure 4 [12].

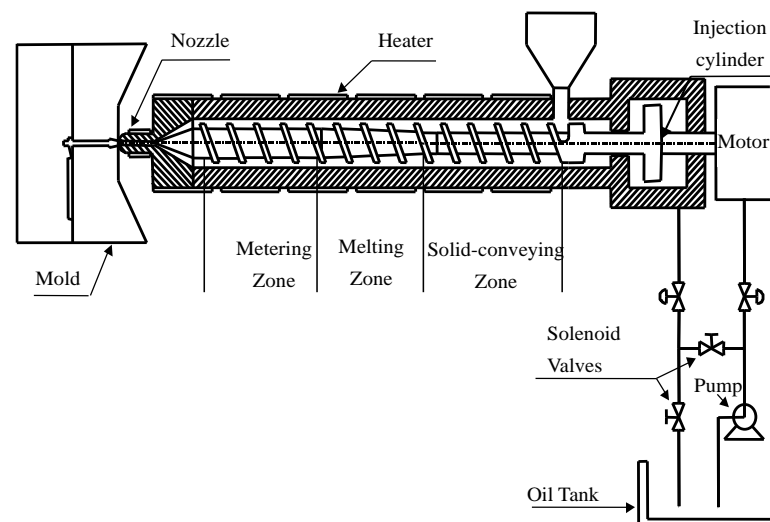


Figure 4. Schematic diagram of the injection molding machine.

According to the characteristics of injection molding processes, the entire injection molding process is divided into four phases, namely the injection phase, the pressure holding phase, the plasticization phase, and the cooling phase. These four phases are considered to be the critical-to-quality operation phases that determine the product quality.

During the injection molding process, many process variables will affect the final product quality, and the values of these process variables can be measured by the corresponding sensors. At the end of each batch, the product quality information, that is, the weight of each product, can also be measured. The key process variables involved in this experiment are listed in Table 1.

Table 1. Process variables of the injection molding process.

No.	Variable Description	Unit
1	Nozzle temperature	°C
2	Screw speed	Mm/s
3	Cylinder pressure	Bar
4	Plasticizing pressure	Bar
5	SV1 valve opening	%
6	SV2 valve opening	%

3.2. Variable Analysis of Injection Molding Process and Experiment Condition

The material used in this work was high-density polyethylene (HDPE), and the specific operating conditions are shown in Table 2 [12]. In the experiment, the sampling information of 100 batches of a real injection molding process was used. Each batch contained 919 sampling points.

Table 2. Operating condition settings for the injection molding process.

Operating Parameter	Set Value
Material	High-density polyethylene (HDPE)
Injection velocity	24 mm/s
Packing pressure	200 bar
Mold cooling water	25 °C
Barrel temperature	230 °C
Packing time	3 s
Cooling time	15 s

Based on the knowledge of the injection molding process, all the sampling points in a batch were divided into four phases. The sample points of the injection phase were samples 1–220; the sample points of the packing–holding phase were samples 221–519; the sample points of the plasticizing phase were samples 520–729; the sample points of the cooling phase were samples 730–919.

The method mentioned in Section 2.2 was used to establish the sliding windows. The number of batches in each window was 30, the sliding step size was $L = 1$, and a total of 71 sliding windows were established.

3.3. Application of Prediction Model and Identification of Related Parameters

3.3.1. Application of One-Dimensional Extended Window Model Using the Samples in KROS Only

A prediction model using k-extended data matrices in the KROS based on sampling time information was constructed within each sliding window using the method mentioned in Section 2. The number of sampling times for the forward extension, F , changed from 0 to 10, and for the c -th phase, the indicator \overline{R}_c^2 values were analyzed to assess the predictive ability of the model and are given in Table 3.

It can be seen that in the different phases, the changing trend of \overline{R}_c^2 roughly increased, and at the same time, this increasing trend gradually slowed down. Therefore, to balance the prediction accuracy and the algorithm complexity, it was necessary to set a threshold ε and to stop the extension when the rate of change was less than this threshold. The expression for the change rate can be written as:

$$\Delta = \frac{\left| \overline{R_{c,F+1}^2} - \overline{R_{c,F}^2} \right|}{\overline{R_{c,F}^2}} \tag{19}$$

where $\overline{R_{c,f}^2}$ represents the value of $\overline{R_c^2}$ in a situation where the extended window includes the $F-1$ forward sampling time for the modeling. If ε is taken as 0.0025, then $F = 6$. Therefore, in the following discussion, F is assigned a value of 6. Taking sliding window 30 and sliding window 50 as examples, the $R_{k,c}^2$ of each sampling time and the mean value of the whole sampling time are given in Figure 5.

Table 3. $\overline{R_c^2}$ based on the k -extended window.

F	Phase 1	Phase 2	Phase 3	Phase 4	Whole
0	0.6674	0.6701	0.7236	0.7551	0.7031
1	0.6735	0.6718	0.7284	0.7590	0.7116
2	0.6784	0.6739	0.7316	0.7621	0.7149
3	0.6834	0.6760	0.7349	0.7648	0.7177
4	0.6881	0.6779	0.7378	0.7668	0.7202
5	0.6924	0.6794	0.7408	0.7687	0.7224
6	0.6961	0.6805	0.7438	0.7699	0.7244
7	0.6993	0.6813	0.7470	0.7709	0.7264
8	0.7021	0.6820	0.7500	0.7714	0.7282
9	0.7046	0.6826	0.7529	0.7718	0.7299
10	0.7068	0.6833	0.7557	0.7720	0.7315

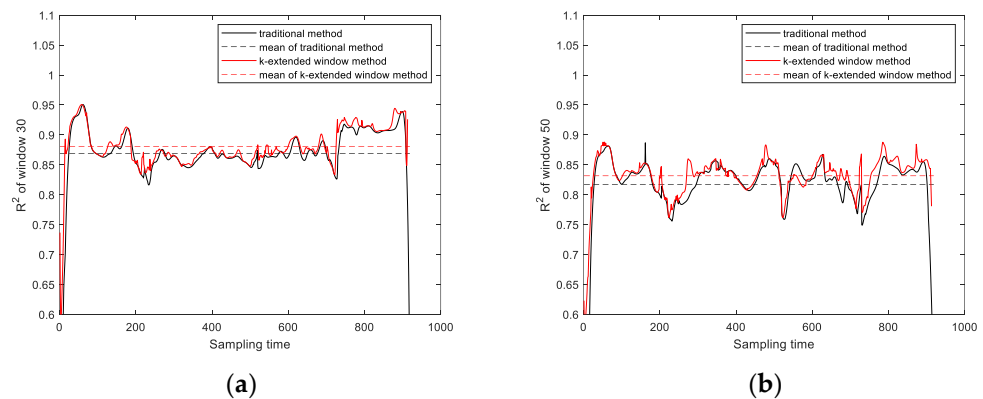


Figure 5. $R_{k,c}^2$ based on the KROS in (a) sliding window 30 and (b) sliding window 50.

Figure 5 shows the performance of the quality prediction model constructed using the traditional method and the method based on the k -extended window method. Here, the traditional method does not consider the ROS. Since, theoretically, all four possible ROSs should be analyzed individually, which is the main contribution of this work, the original two ROSs are not analyzed as a unit. As can be seen in Figure 5, using the extended window modeling in the sampling time direction, from the perspective of sampling times, the average performance was boosted, and most $R_{k,c}^2$ values of the sampling points were improved. The discussion above verifies the rationality of the proposed method based on the k -extended window method.

3.3.2. Application of Extended Window Model Using the Samples in IROS and KIROS

Similarly, the prediction model using the i -extended data matrices in the IROS based on batch information was constructed within each sliding window using the method mentioned in Section 2, as well as the prediction model using the k - i -extended data matrices in the KIROS. The number of sampling times for the forward extension, F , was uniformly set to 0 and 6, and on this basis, the number of extended batches, N , changed from 0 to 10.

The indicator $\overline{R_c^2}$ values were analyzed to assess the predictive ability of the model and are given in Table 4.

Table 4. $\overline{R_c^2}$ based on the k -extended window and k - i -extended window.

F	N	Phase 1	Phase 2	Phase 3	Phase 4	Whole
0	0	0.6674	0.6701	0.7236	0.7551	0.7031
	1	0.7125	0.6948	0.7781	0.7727	0.7281
	2	0.7620	0.7526	0.8180	0.8193	0.7596
	3	0.7951	0.8070	0.8458	0.8323	0.7934
	4	0.8359	0.8280	0.8686	0.8445	0.8129
	5	0.8585	0.8591	0.8911	0.8641	0.8332
	6	0.8723	0.8795	0.8915	0.8788	0.8468
	7	0.8903	0.8879	0.7827	0.9014	0.8576
	8	0.9011	0.9063	0.8121	0.9119	0.8709
	9	0.9098	0.9165	0.8271	0.9203	0.8804
	10	0.9192	0.9196	0.8392	0.9252	0.8850
6	0	0.6961	0.6805	0.7438	0.7699	0.7244
	1	0.7343	0.6987	0.7977	0.7904	0.7409
	2	0.7785	0.7578	0.8393	0.8313	0.7699
	3	0.8088	0.8115	0.8652	0.8419	0.8033
	4	0.8465	0.8321	0.8841	0.8538	0.8214
	5	0.8669	0.8628	0.9050	0.8726	0.8409
	6	0.8799	0.8830	0.9023	0.8863	0.8540
	7	0.8974	0.8910	0.7886	0.9085	0.8649
	8	0.9072	0.9095	0.8175	0.9178	0.8778
	9	0.9154	0.9193	0.8312	0.9256	0.8868
	10	0.9246	0.9223	0.8423	0.9295	0.8913

It can be easily seen in the table that the $\overline{R_c^2}$ values roughly increased, and at the same time, the increase rates gradually decreased. Here, the threshold ε was 0.015, and N was set to 5. From the above table, the following conclusions can be drawn. First, when 10 batches were extended downward, the $\overline{R_c^2}$ values of Phase 1, Phase 2, and Phase 4 all reached more than 0.9. Compared to the extended window in the sampling time direction, the extended window in the batch direction achieved a better prediction effect. Second, comparing the cases where F was 0 and F was 6 in the table, it was found that the $\overline{R_c^2}$ of the latter was higher than the former under the condition of the same batch extension quantity. That is, when the windows in the direction of both the sampling time and the batch were used in combination, the effect was superimposed. This illustrates the rationality of constructing a two-dimensional extended window based on time-batch evolution information. Window 30 and window 50 were also selected to obtain the $R_{k,c}^2$ values of each sampling time, as shown in Figure 6.

Figure 6 shows the performance of the quality prediction model constructed using three methods: the traditional method, the method based on the i -extended window, and the method based on the k - i -extended method. It can be seen in Figure 6 that the $R_{k,c}^2$ values at most of the sampling points were improved due to the construction of the extended window. Furthermore, the $R_{k,c}^2$ values of the two-dimensional extended window were better than that of the one-dimensional extended window. In addition, it can be observed that the gain in $R_{k,c}^2$ due to the extension of the sampling time direction was significantly smaller than that of the extended batch. In the injection molding process, the correlation between two neighboring batches is relatively strong, which is in line with relevant production knowledge. In conclusion, the above discussion justifies the prediction method based on the i -extended window and the k - i -extended window.

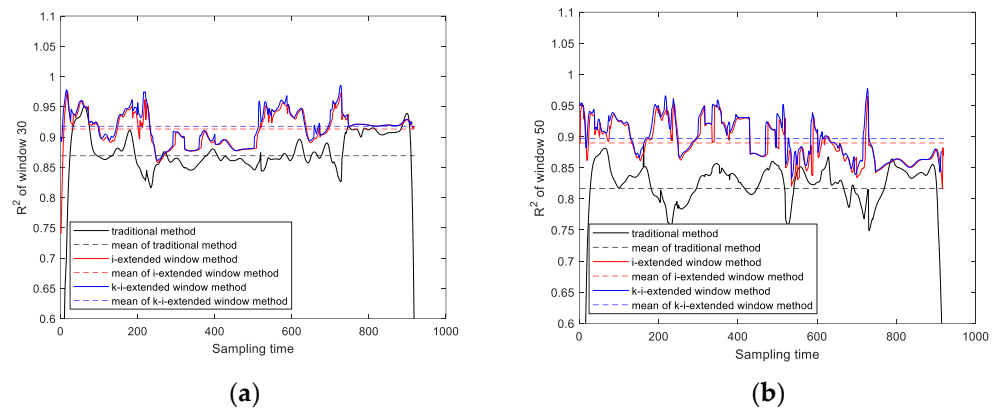


Figure 6. $R^2_{k,c}$ based on the IROS and KIROS in (a) sliding window 30 and (b) sliding window 50.

3.3.3. Application of Extended Window Prediction Model Using the Samples in BROS

The method described in Section 2.3 was used to construct an extended window based on the backward time information of historical batches. During the analysis, the number of backward sampling times for backward extension, B , varied from 0 to 10. At the same time, the additivity of the extension in the batch direction was studied, and the number of expanded batches, N , was set to 1 and 5. The $\overline{R^2_c}$ values are given in Table 5.

Table 5. $\overline{R^2_c}$ values based on the back-extended window.

F	B	Phase 1	Phase 2	Phase 3	Phase 4	Whole
1	0	0.7125	0.6948	0.7781	0.7727	0.7281
	1	0.7084	0.6903	0.7745	0.7678	0.7268
	2	0.7062	0.6873	0.7726	0.7659	0.7273
	3	0.7044	0.6851	0.7719	0.7662	0.7279
	4	0.7050	0.6836	0.7718	0.7682	0.7288
	5	0.7069	0.6829	0.7721	0.7702	0.7299
	6	0.7093	0.6827	0.7724	0.7724	0.7311
	7	0.7117	0.6829	0.7729	0.7743	0.7322
	8	0.7140	0.6833	0.7735	0.7759	0.7334
	9	0.7162	0.6841	0.7741	0.7773	0.7343
5	10	0.7179	0.6849	0.7748	0.7782	0.7349
	0	0.8585	0.8591	0.8911	0.8641	0.8332
	1	0.8503	0.8528	0.8890	0.8564	0.8277
	2	0.8467	0.8482	0.8879	0.8529	0.8251
	3	0.8450	0.8460	0.8875	0.8507	0.8244
	4	0.8443	0.8448	0.8879	0.8488	0.8245
	5	0.8443	0.8442	0.8885	0.8471	0.8250
	6	0.8449	0.8439	0.8897	0.8455	0.8257
	7	0.8460	0.8439	0.8910	0.8443	0.8266
	8	0.8475	0.8441	0.8925	0.8432	0.8275
9	0.8493	0.8444	0.8941	0.8422	0.8285	
10	0.8512	0.8448	0.8957	0.8414	0.8296	

The following conclusions can be drawn from the above table. For the proposed backward extended window, the $\overline{R^2_c}$ decreased in the initial stage of the gradual increase in the extension point. After about five sampling times, the $\overline{R^2_c}$ began to rise. In some cases, the $\overline{R^2_c}$ increased rapidly until it exceeded the initial state, such as $N = 0$, Phase 1, while some increased slowly. First, the decrease in the $\overline{R^2_c}$ in the initial situation occurred. As proposed in the method, since the data after the k -th sampling time of the current i -th batch could not be obtained during the online quality prediction, to fill in the missing data, the corresponding time information of the $(i - 1)$ -th batch was selected to replace these

missing data. This approximate substitution resulted in a slight loss in the $\overline{R_c^2}$. As a result of this substitution, the time correlation of the process variable data with the quality data of the current batch was reduced. This phenomenon became more obvious as the extended batch increased, which can be seen in the comparison between $N = 1$ and $i = 5$. However, as the number of backward sampling times included continued to increase, the $\overline{R_c^2}$ value gradually increased. In some cases, an extension of fewer than 10 sampling times exceeded the initial situation, which proves that the backward moment is indeed related to the currently considered sampling time. The positive effect of the backward extended window is reflected. Combined with the technological characteristics of the injection molding process, the reasons for this phenomenon are explained as follows. During the backward extension, the sampling k -th time involved gradually increases. As the data increase, they become obviously closer to the current batch, and the correlation becomes stronger. At the same time, with the continuous growth at the data scale, the relationship between the process variables becomes gradually significant. These two effects gradually recover the $\overline{R_c^2}$ values of the prediction model. As for the differences in the growth speed among the different phases, they are related to the differences among the phases in the actual injection molding process. Finally, the suitable size of the proposed backward extended window was obtained. Through the extension of the backward sampling time of the historical batch, with the continuous addition of sampling points, the $\overline{R_c^2}$ values show an unstable upward trend. In other words, unlike the forward extension discussed earlier, the trend of the $\overline{R_c^2}$ changes in this case did not appear to slow down significantly. The reason is that the backward sampling points on the historical batches are all relatively far apart for the k -th sampling time of the i -th batch considered when modeling. This long distance weakens the difference between the backward extension points. Therefore, in the process of continuous extension, the goodness of fit can be uniformly larger. In addition, the sampling time k^* of the historical batch was observed. Because batches of the injection molding process are carried out successively, when k^* is far from k , it is closer to batch i ; when k^* is close to k , it is farther from batch i . This shows that there is a check-and-balance relationship between the sampling time and the batch, which brings additional uncertainty and, therefore, leads to an increase in goodness-of-fit fluctuations. Based on the above discussion, a larger point of the backward extension performs better. The main purpose was to overcome the negative impact caused by the extension points that were too small. At the same time, to consider the complexity of the algorithm, the number of backward extensions was selected as 10.

Window 30 and window 50 were also selected to obtain the $R_{k,c}^2$ of each sampling point using the traditional method, the backward extended window method with one extended batch, and the backward extended window method with five extended batches. The results are shown in Figure 7.

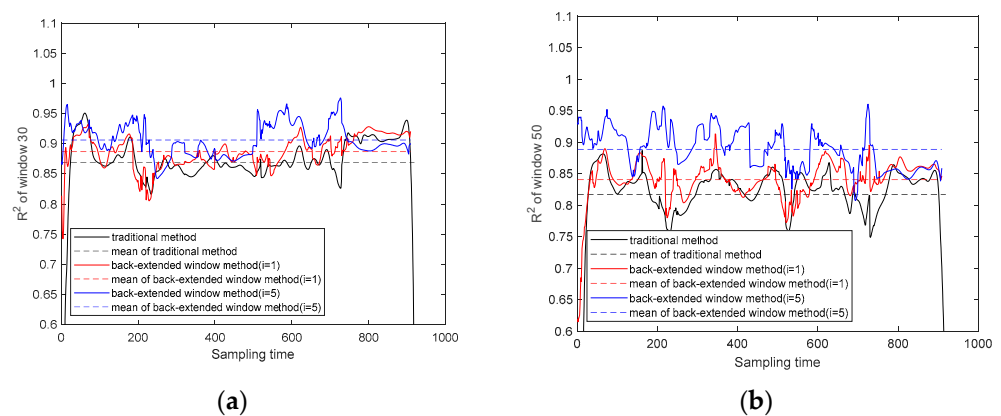


Figure 7. $R_{k,c}^2$ based on the BROS in (a) sliding window 30 and (b) window 50.

As shown in Figure 7, compared to those of the traditional method, the $R_{k,c}^2$ values of the model built using the back-extended window were improved; at the same time, when

more batches were expanded, the $R_{k,c}^2$ values of the model improved. This matches the conclusion obtained previously; that is, the backward extension of the data at the sampling time can help to improve the prediction model. The benefits obtained by the extension of the batch and the extension of the backward sampling times can also be superimposed.

3.3.4. Application of the k - i -Back-Extended Window Model

In this section, the rationality of the k - i -back-extended window based on the time-batch evolution information is verified. The sets of parameter combinations are listed in Table 6, and the corresponding $\overline{R_c^2}$ values are analyzed separately.

Table 6. Sets of parameter combinations and corresponding $\overline{R_c^2}$ values.

No.	F	N	B	$\overline{R_c^2}$
1	0	0	0	0.6539
2	6	0	0	0.6827
3	0	5	0	0.8493
4	0	1	6	0.6941
5	6	5	0	0.8584
6	6	1	6	0.7229
7	0	5	6	0.8376
8	6	5	6	0.8646

It can be seen in Table 6 that with the continuous extension of the data, the $\overline{R_c^2}$ values continue to increase, which proves that the $\overline{R_c^2}$ obtained using the extension in the various directions discussed above can be continuously increased.

3.4. Online Quality Analysis and Prediction

Online quality prediction was conducted using the proposed model prediction method based on the time-batch evolution information. For a better comparison, in addition to using the proposed k - i -back-extended window model, the traditional method, the k -extended window method, the i -extended window method, the k - i -extended window method, and the back-extended window method were used to perform the task of quality prediction. The parameter settings for these experiments are shown in the Table 7.

Table 7. Quality prediction methods used for comparison.

Method	F	N	B
Traditional	0	0	0
k -extended window	6	0	0
i -extended window	0	5	0
k - i -extended window	6	5	0
back-extended window	0	1	10
k - i -back-extended window	6	5	10

An analysis was also performed using the sliding windows, and the middle batch of each window was selected as the test batch to verify the accuracy of each prediction method. First, to analyze the stability of the prediction model with the proposed ROS, four typical test batches were chosen to present the online prediction results. For the four test batches, online quality prediction was performed, and the predicted weight results obtained using the six methods at each sampling time are plotted in Figure 8.

It can be clearly seen in Figure 8 that the prediction performance of the traditional method was more unstable compared to the proposed methods based on extended windows, especially in window 51 and window 71. The prediction results of the proposed method are more stable than the traditional method; that is, the prediction methods of the four extended window models based on the proposed method are significantly better than

the traditional method regarding stability. To further understand the accuracy gained using the proposed four models, the mean RMSE values corresponding to all the sampling times in each test batch are listed in Table 8.

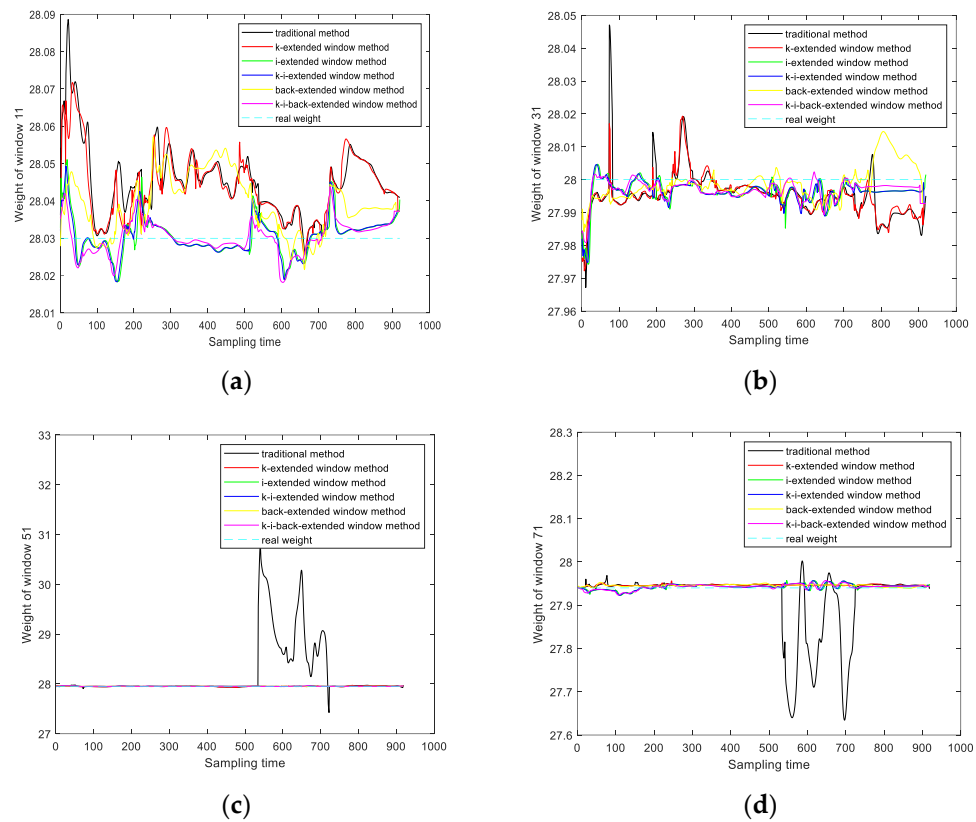


Figure 8. Predicted results of each sampling time in (a) sliding window 11, (b) sliding window 31, (c) sliding window 51, and (d) sliding window 71.

Table 8. Comparison of RMSE values gained using the different prediction methods.

Method	Batch 11	Batch 31	Batch 51	Batch 71	Mean
Traditional	0.0151	0.0046	0.2318	0.0224	0.0685
<i>k</i> -extended window	0.0141	0.0049	0.0016	0.0064	0.0068
<i>i</i> -extended window	6.516×10^{-4}	0.0037	0.0031	0.0027	0.0025
<i>k-i</i> -extended window	5.403×10^{-4}	0.0037	0.0032	0.0027	0.0025
back-extended window	0.0092	0.0014	0.0031	0.0055	0.0048
<i>k-i</i> -back-extended window	2.587×10^{-4}	0.0031	0.0039	0.0024	0.0024

It can be seen that in the selected test batches given above, the prediction method based on the *k-i*-back-extended window generally achieved the best results. The prediction method based on this kind of extended window had the lowest RMSE on average. In the 11th window, its RMSE indicator reached a low value of 2.587×10^{-4} . In addition, it should be noted that in the four methods for each test batch, the RMSE could only reach the lowest value with an extension in the direction of the sampling time. But this advantage is obviously unstable. For example, for batch 31, the prediction model that only used the sampling time to extend the window was not even as good as the traditional method. In other words, when only a one-dimensional extension is performed, the accuracy advantage may only be obtained in individual test batches. Based on the above, the effects of the five methods proposed in this paper on quality prediction were proven.

Therefore, combining the $\overline{R_c^2}$ index and $R_{k,c}^2$ index obtained in the previous section, the following conclusions can be drawn. Firstly, compared to the traditional method, an

extension in the direction of the batches or in the direction of the historical sampling time can achieve the purpose of improving the accuracy, and an extension in either the sampling time or batch direction is meaningful. Secondly, by considering the evolution information of the two directions in the model at the same time, the establishment of an extended window based on the time-batch evolution information of the sampling in both directions can further improve the accuracy and effectively improve the stability of the prediction model. In addition, in the actual production process, several modeling methods based on the extended window proposed above are suggested. When the production is in pursuit of the obtainment of high-precision products quickly and easily, it is recommended to use the one-dimensional extended window. When the production accuracy requirement is very high, then the two-dimensional windows should be used to build quality prediction models.

4. Conclusions

This paper proposes a new quality prediction strategy for batch processes. In the proposed method, newly defined ROSs are used to build five different extended windows, which contain the data information of historical batches and historical sampling times. The quality prediction models of these extended windows have richer batch-time operation evolution information, and the evolution information results in higher prediction accuracy. When all the sampled data in the KIBROS is considered in the model, the k - i -back-extended window is established, and the highest accuracy is obtained in the application to the injection molding process. For complex production situations, when product quality accuracy is critical, the two-dimensional KIBROS extended window is recommended. However, the application background of this work is the injection molding process, where sample data are limited. Although the representative multivariable statistical method, PLS, offered satisfactory modeling results in this work, deep learning methods are also recommended for general processes with a large amount of data to adapt the method to real-time monitoring and control applications.

Author Contributions: Conceptualization, L.Z.; methodology, L.Z. and J.Y.; software, J.Y.; validation, J.Y.; formal analysis, J.Y.; investigation, J.Y.; resources, L.Z.; data curation, L.Z.; writing—original draft preparation, L.Z. and J.Y.; writing—review and editing, L.Z.; visualization, J.Y.; supervision, L.Z.; project administration, L.Z.; funding acquisition, L.Z. All authors have read and agreed to the published version of the manuscript.

Funding: This research was funded by the National Natural Science Foundation of China (No. 61503069) and the Fundamental Research Funds for the Central Universities (N2404010).

Data Availability Statement: The data will be made available by the authors on request.

Conflicts of Interest: The authors declare no conflicts of interest.

References

1. Dunteman, G. *Principal Component Analysis*; SAGE Publication Inc.: Los Angeles, CA, USA, 1989.
2. Geladi, P.; Kowalshi, B. Partial least squares regression: A tutorial. *Anal. Chim. Acta* **1986**, *185*, 1–17. [[CrossRef](#)]
3. Wang, X. *Data Mining and Knowledge Discovery for Process Monitoring and Control*; Springer: Berlin/Heidelberg, Germany, 1999.
4. Kourti, T.; MacGregor, J. Process analysis, monitoring and diagnosis, using multivariate projection methods. *Chemom. Intell. Lab. Syst.* **1995**, *28*, 3–21. [[CrossRef](#)]
5. Wang, H. *Partial Least Squares Regression Method and Its Application*; National Defense Industry Press: Beijing, China, 1999.
6. Nomikos, P.; MacGregor, J. Monitoring batch processes using multiway principal component analysis. *AIChE J.* **1994**, *40*, 1361–1375. [[CrossRef](#)]
7. Nomikos, P.; MacGregor, J. Multi-way partial least squares in monitoring batch processes. *Chemom. Intell. Lab. Syst.* **1995**, *30*, 97–108. [[CrossRef](#)]
8. Wold, S.; Kettaneh, N.; Fridén, H.; Holmberg, A. Modelling and diagnostics of batch processes and analogous kinetic experiments. *Chemom. Intell. Lab. Syst.* **1998**, *44*, 331–340. [[CrossRef](#)]
9. Duchesne, C.; MacGregor, J. Multivariate analysis and optimization of process variable trajectories for batch process. *Chemom. Intell. Lab. Syst.* **2000**, *51*, 125–137. [[CrossRef](#)]
10. Cho, H.; Kim, K. A method for predicting future observations in the monitoring of a batch process. *Qual. Technol.* **2003**, *35*, 59–69. [[CrossRef](#)]

11. Lu, N.; Wang, F.; Gao, F. Sub-PCA modeling and online monitoring strategy for batch processes. *AIChE J.* **2004**, *50*, 255–259. [[CrossRef](#)]
12. Zhao, L.; Zhao, C.; Gao, F. Inter-batch-evolution-traced process monitoring based on inter-batch mode division for multi-phase batch processes. *Chemom. Intell. Lab. Syst.* **2014**, *138*, 178–192. [[CrossRef](#)]
13. Zhao, L.; Wang, F.; Chang, Y.; Wang, S.; Gao, F. Phase-based recursive regression for quality prediction of multi-phase batch processes. In Proceedings of the 13th IEEE International Conference on Control and Automation, Ohrid, Macedonia, 3–6 July 2017; pp. 283–288.
14. Hwang, D.; Han, C. Real-time monitoring for a process with multiple operating modes. *Control Eng. Pract.* **1999**, *7*, 891–902. [[CrossRef](#)]
15. Chen, J.; Liu, J. Mixture principal component analysis models for process monitoring. *Ind. Eng. Chem. Res.* **1999**, *38*, 1478–1488. [[CrossRef](#)]
16. Zhao, L.; Zhao, C.; Gao, F. Between-mode quality analysis based multi-mode batch process quality prediction. *Ind. Eng. Chem. Res.* **2014**, *53*, 15629–15638. [[CrossRef](#)]
17. Zhao, L.; Huang, X. Slow time-varying batch process quality prediction based on batch augmentation analysis. *Sensors* **2022**, *22*, 512. [[CrossRef](#)] [[PubMed](#)]
18. Zhao, L.; Huang, X.; Yu, H. Quality-analysis-based process monitoring for multi-phase multi-mode batch processes. *Processes* **2021**, *9*, 1321. [[CrossRef](#)]
19. Zhao, L.; Yang, J. Batch process monitoring based on quality-related time-batch 2D evolution information. *Sensors* **2022**, *22*, 2235. [[CrossRef](#)] [[PubMed](#)]
20. Zhao, L.; Huang, X. Two-dimensional, two-layer quality regression model based batch process monitoring. *Processes* **2022**, *10*, 43. [[CrossRef](#)]
21. Yao, Y.; Lu, N.; Gao, F. Two-dimensional dynamic PCA with auto-selected support region. *IFAC Proc. Vol.* **2007**, *40*, 69–74. [[CrossRef](#)]
22. You, L.X.; Chen, J. Autogenerated multilocal PLS models without pre-classification for quality monitoring of nonlinear processes with unevenly distributed data. *Ind. Eng. Chem. Res.* **2022**, *16*, 5898–5913. [[CrossRef](#)]
23. Zou, M.; Zhao, L.; Wang, S.; Chang, Y.; Wang, F. Quality analysis and prediction for start-up process of injection molding processes. *IFAC PapersOnLine* **2018**, *51*, 233–238. [[CrossRef](#)]
24. Jia, R.; Mao, Z.; Wang, F. KPLS model based product quality control for batch processes. *CIESC J.* **2013**, *64*, 1332–1339.

Disclaimer/Publisher’s Note: The statements, opinions and data contained in all publications are solely those of the individual author(s) and contributor(s) and not of MDPI and/or the editor(s). MDPI and/or the editor(s) disclaim responsibility for any injury to people or property resulting from any ideas, methods, instructions or products referred to in the content.